Aromatic poly(fluorocarbinol)s: soluble, hydrophobic binders for inkjet formulations

Aromatic poly(fluorocarbinol)s: Soluble, hydrophobic binders for inkjet formulations

Jessica Godleman,[a] Flavien Leroux,[a] Stuart Reynolds,[b] Julian Philpott,[b] Philippa B. Cranwell,[a] Josephine L. Harries,[b] Wayne Hayes*[a] and Howard M. Colquhoun*[a]

[a]Department of Chemistry, University of Reading, Whiteknights, Reading, RG6 6DX, U.K. e-mail: h.m.colquhoun@reading.ac.uk, w.c.hayes@rdg.ac.uk. Tel: +44 118 378 6491

[b]Domino UK Ltd, Trafalgar Way, Bar Hill, Cambridge, CB23 8TU, U.K.

Abstract

Aromatic poly(fluorocarbinol)s with molecular weights (M_n) in the range 11,000–115,000 g mol^{-1}) have been synthesised and their potential as polymeric binders in ink formulations for deposition by continuous inkjet (CIJ) printers investigated. A small scale, proof of concept study, using a drop-on-demand inkjet printer, suggested that the three lowest molecular weight polymers (M_n = 11,500 – 25,200 g mol^{-1}) could behave as very good binders in this type of application. Two of these poly(fluorocarbinol)s (M_n = 11,500 and 25,200 g mol^{-1}) were analysed as MEK solutions, pre-deposition, using shear-flow rheology. The lower-MW material exhibited Newtonian fluid characteristics whereas the higher-MW polymer behaved as a non-Newtonian fluid. For CIJ printing, both polymers were formulated in MEK using Orasol Orange®, an ionic cobalt dye-complex, to visualise the prints and provide a charge for deflection of ink droplets. The resulting solutions were deposited successfully on a variety of different packaging substrates using a CIJ printhead, resulting in high-resolution printed code. Magnified views of the jetstream during printing showed well-defined droplet formation without any evident satellite drops. These polymeric binders showed limited adhesion to low density poly(ethylene) (LDPE) and polypropylene (PP) surfaces, but moderately good adhesion to steel and excellent adhesion to poly(ethylene terephthalate) (PET), nylon-6,6 and glass. Contact angle measurements on drawn-down films of these poly(fluorocarbinol)s showed that, despite their ready solubility in high-polarity solvents such as alcohols and ketones, poly(fluorocarbinol)s afford coatings with relatively hydrophobic surfaces (water contact angles ca. 90°). Such polymers thus appear to be excellent candidates for binders in inkjet formulations, with materials having M_n in the range 10,000 to 25,000 g mol^{-1} displaying properties that are very well suited to use in continuous inkjet deposition for coding and marking on an industrial scale.

1. Introduction

Coding and marking of manufactured products by inkjet printing is an established and important procedure, involving the printing of information such as batch numbers, location of manufacture and expiration dates that, in turn, allow ready identification of products and their production path. Durability of the print is of utmost importance as it ensures that the information is legible throughout the required lifetime of the packaged product, but this is not always achievable using formulations containing only a carrier solvent and a pigment or dye. Polymeric binders are thus included in many inkjet formulations and provide beneficial properties both during and after deposition [1]. In particular, a low concentration of a polymer in an inkjet formulation can aid efficient droplet formation and reduce the generation of satellite droplets [1–4], which, in turn, improves the resolution of the printed code. Polymers are also used to modify the formulation viscosity [5], improve pigment dispersion [1,2,6] and, as noted above, increase the durability of the printed code [2,7].

However, despite the enhanced properties gained by the incorporation of polymeric binders in inkjet formulations, the use of high concentrations of polymers or other very high molecular weight materials can adversely affect drop generation and ejection from the nozzle [3,4,8]. Careful selection of the polymeric binder is thus required to achieve optimum post-deposition properties while also affording precise droplet formation with minimal generation of satellite drops. Polymeric binders also need to demonstrate good solubility in the high-polarity solvents used in inkjet formulations, yet also demonstrate a degree of surface-hydrophobicity to improve the durability of the print.

Polymers containing trifluoromethyl groups often exhibit segregation of these groups at the polymer-air interface [9], resulting in films with hydrophobic surfaces [9–14]. For example, Banerjee *et al*. reported a series of copolymers produced by free-radical copolymerization of 2,2,2-trifluoroethyl α-fluoroacrylate (FATRIFE) with different ratios of 2-(trifluoromethyl)acrylic acid (MAF), affording a series of poly(FATRIFE-*co*-MAF) materials whose hydrophobic characteristics decreased as the carboxylic acid (MAF) content increased [10]. The incorporation of trifluoromethyl groups into polymer structures can also aid solubility. Liu *et al*. [14] reported the synthesis of aromatic poly(ether ketone)s, (PEKs), both with and without 3-trifluoromethylphenyl substituents and showed that inclusion of the trifluoromethylphenyl groups enhanced the solubility of the polymers in organic solvents such as THF, DMF, DMAc or NMP when compared to non-fluorinated PEK derivatives [14].

Although trifluoromethylated polymers may exhibit hydrophobic character when deposited as films, the solubility of such polymers in solvents of high polarity can be either very poor or even non-existent, rendering the materials useless for inkjet deposition purposes. However, the solubility of fluoropolymers in high-polarity solvents could be improved by the incorporation of strongly polar groups into the polymer architecture to produce materials that contain both hydrophilic and hydrophobic functionalities. Aromatic poly(fluorocarbinol)s [15] address these structural characteristics as they feature both a trifluoromethyl group and an hydroxy residue appended to the same carbon centre within the repeat unit of the polymer. Leroux *et al*. recently reported the synthesis of a series of poly(fluorocarbinol)s that exhibit excellent solubility in high-polarity solvents such as acetone, methanol (MeOH), ethanol (EtOH) and *iso*-propanol (*i*-PrOH) [16]. Despite the inherently high polarity of these poly(fluorocarbinol)s, the surfaces of their cast films exhibited hydrophobic properties with water contact angles of ~90°. The hydrophobicity of the films was attributed to spontaneous enrichment of the polymer-air interface with trifluoromethyl groups, and this was confirmed by X-ray photoelectron spectroscopic analysis. Here we report an investigation into the development and application of the aromatic poly(fluorocarbinol) **1** (Figure 1) as a new polymeric binder for use in inkjet printing formulations.

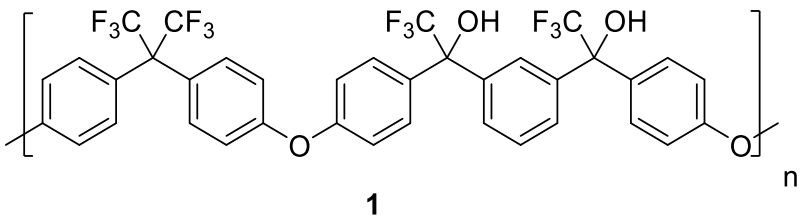

1

Figure 1. Molecular structure of the poly(fluorocarbinol) investigated in this work.

2. Results and discussion

2.1 Polymer synthesis and characterisation

This study used the three-step synthetic route reported by Leroux *et al*. [16] (Scheme 1) to generate a series of poly(fluorocarbinol)s (PFOs) **1a-e**. This route involved first the synthesis of poly(ether diketone)s (PEKKs) **2a-e,** employing different feed ratios of 4,4'-hexafluoro(*iso*propylidene)diphenol (**3)** and 1,3'-bis(fluorobenzoyl)benzene (**4)** to control the final molecular weight. See Table 1 for molecular weight data, and the Supplementary Data (SD) for more detailed characterisation of these polymers (Figures S1-S11).

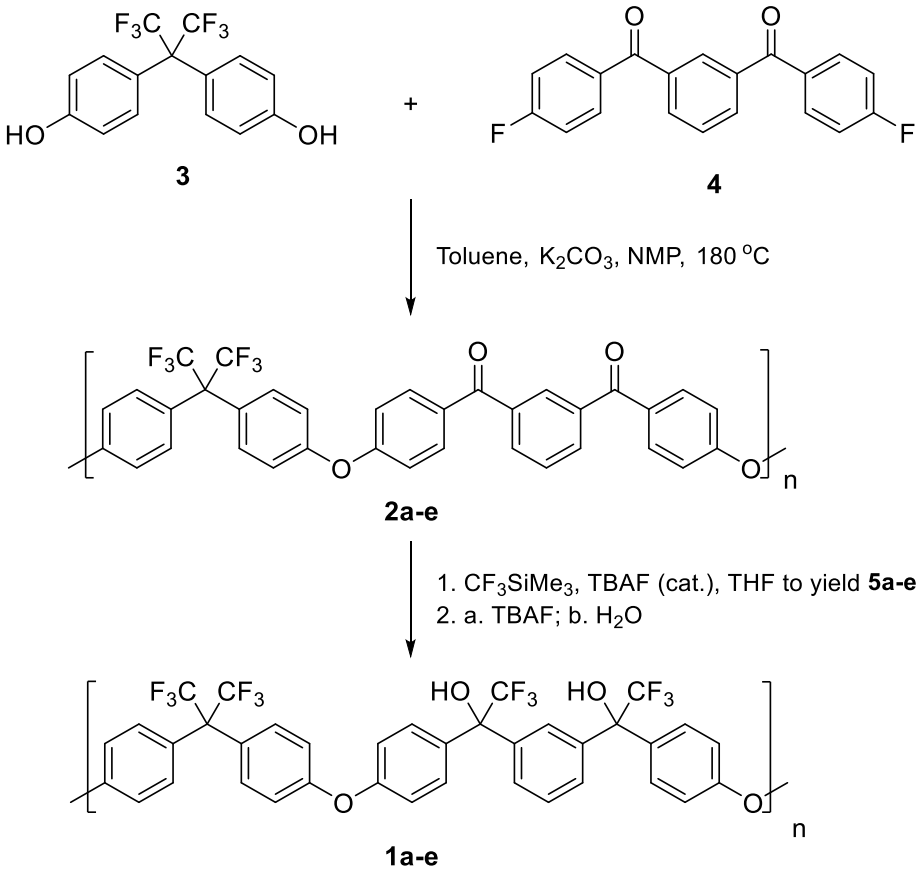

Scheme 1. The three-step synthetic route used to obtain PFOs **1a-e** (see also SD).

Table 1. Calculated (from monomer feed-ratios) and observed molecular weights (M_n) of samples of PEKK **2**, produced using different feed ratios of monomers **3** and **4**.

Polymer number	Monomer 3 feed	Monomer 4 feed	Calc. X_n	Calc. M_n (g mol^{-1})	Observed M_n (g mol^{-1}) GPC
2a	1.0	1.0	∞	∞	114,000
2b	0.9	1.0	19	11,800	10,500
2c	0.925	1.0	26	16,000	15,600
2d	0.95	1.0	39	24,000	22,000
2e	0.975	1.0	79	42,500	42,500

The diketone monomer 1,3'-bis(fluorobenzoyl)benzene (**3)** was chosen to afford PEKKs **2a-e** with two ketone functionalities per repeat unit; subsequent conversion to PFOs **1a-e** would thus yield materials with two fluorocarbinol units, rather than one, per repeat unit. It was envisaged that this design feature would enhance the solubility of the polymer in polar solvents such as MEK and thus allow ready formulation of the polymer into inkjet inks. Polyketones **2a-e** were converted to the resultant poly(trifluoromethyl silyl ether)s **5a-e** (Figures S12-S27), by reaction with Ruppert's reagent, CF_3SiMe_3 [16–21], catalysed by tetra-*n*-butylammonium fluoride (TBAF). The PSEs were then reacted with an excess of TBAF to produce the desired PFOs **1a-e** (Figures S28-S42). Thus, for example, an exact 1:1 molar feed-ratio of **3** and **4** gave a very high molecular weight poly(ether diketone) (PEKK **2a**, M_n = 114,000 g mol^{-1}), with a dispersity of 2.29 and a glass transition temperature of 162 °C. Trifluoromethylation of PEKK **2a** as outlined above led to high molecular weight PFO **1a** (114,500 g mol^{-1}) which proved readily soluble in a variety of organic solvents of high polarity, including: MEK, acetone, THF, $CHCl_3$, CH_2Cl_2, MeOH, EtOH, and i-PrOH. The observed molecular weights of the resulting PFOs, (M_n = 11,500, 19,100, 25,200 and 44,900 g mol^{-1} for **1b**–**e**, respectively); (Figure 2) were in very good agreement with their predicted molecular weights, after conversion (Scheme 1) from the corresponding polyketones **2b-2e**.

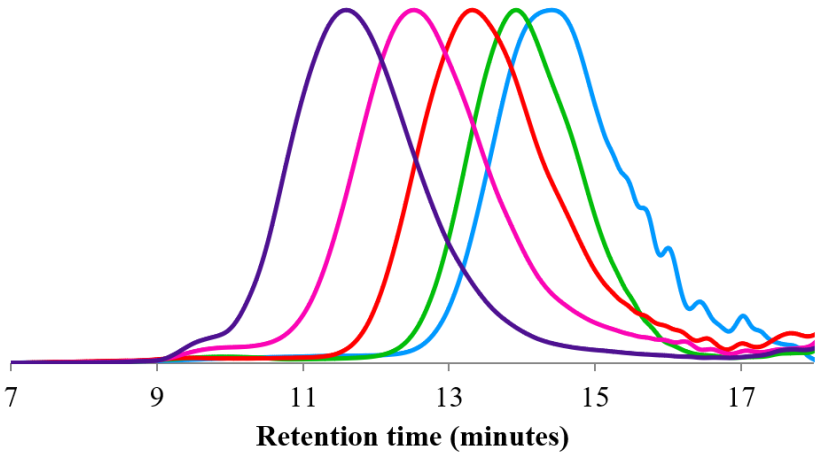

PFO	M_n	M_w	$Đ$
1a	114,500	254,800	2.22
1b	11,500	19,400	1.68
1c	19,100	28,600	1.54
1d	25,200	46,400	1.84
1e	44,900	101,600	2.27

Figure 2. GPC chromatograms for molecular weight controlled PFOs, showing the increase in molecular weight from **1b–1e**. GPC analyses were carried out in THF at polymer concentrations of 2 mg mL^{-1}.

As anticipated, decreasing the molecular weight of the poly(fluorocarbinol)s resulted in a decrease in the glass transition temperature of these materials. The highest-MW PFO, **1a,** produced using an exact 1:1 ratio of monomers **3** and **4**, exhibited a glass transition temperature of 141 °C whereas DSC analysis of the lower molecular weight polymers **1b**–**e** showed significantly lower glass transition temperatures, in the range 114–134 °C (Figure S43).

2.2 Contact angles and surface energies

Despite the ready solubility of PFO **1a** in high-polarity solvents, films cast from solution demonstrated hydrophobic surface-properties. To investigate these properties, films of PFO **1a** were produced at ambient temperature by casting, drawing down, and evaporating a 5% solution of **1a** in MEK, using a 24 µm K-bar, to produce even films of thickness *ca*. 1.2 µm after evaporation of the solvent. Films of PFO **1a** were produced on glass, stainless steel,

PET, nylon 6,6, LDPE and PP. The hydrophobicity of each polymer film was determined via contact angle analysis, with the contact angles of water droplets on both coated and uncoated substrates being measured with an optical tensiometer in sessile drop mode. The sessile drop method suspended 5 µL water droplets from the solvent nozzle, before manual agitation forced the droplet from the nozzle and onto the substrate. The angles of the droplet were recorded every 0.1 seconds over a period of 20 seconds, after which time the surface droplet had ceased spreading (Figure 3).

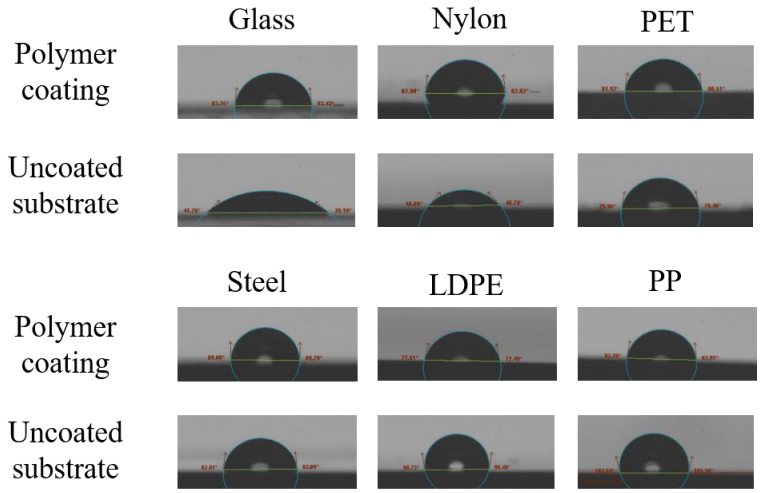

Figure 3. Water droplets on uncoated glass, nylon 6,6, PET, stainless steel, LDPE and PP substrates, together with images of the same substrates coated with PFO **1a**, demonstrating the changes in contact angle on coating.

This analysis revealed some significant changes in the contact angle of water droplets on the PFO-coated substrates when compared to the uncoated substrates. Uncoated glass and nylon showed very low contact angles of 41° and 49° respectively, indicating strongly hydrophilic surfaces. However, the contact angles increased sharply to 83° and 84° respectively on coating with PFO **1a**, indicating the production of moderately hydrophobic surfaces. Uncoated stainless steel, LDPE and PP exhibited non-polar surfaces, with water contact angles of 90°, 99° and 104°, and these substrates exhibited a decrease in water contact angle on coating, to 84°, 76° and 80° respectively. PET showed little change in contact angle on coating, indicating similar surface polarities of PET and PFO **1a**. The relative hydrophobicity of the polymer film surfaces, despite the bulk polarity of the polymer, is attributed to preferential segregation of CF_3 groups at the polymer-air interface [9-14].

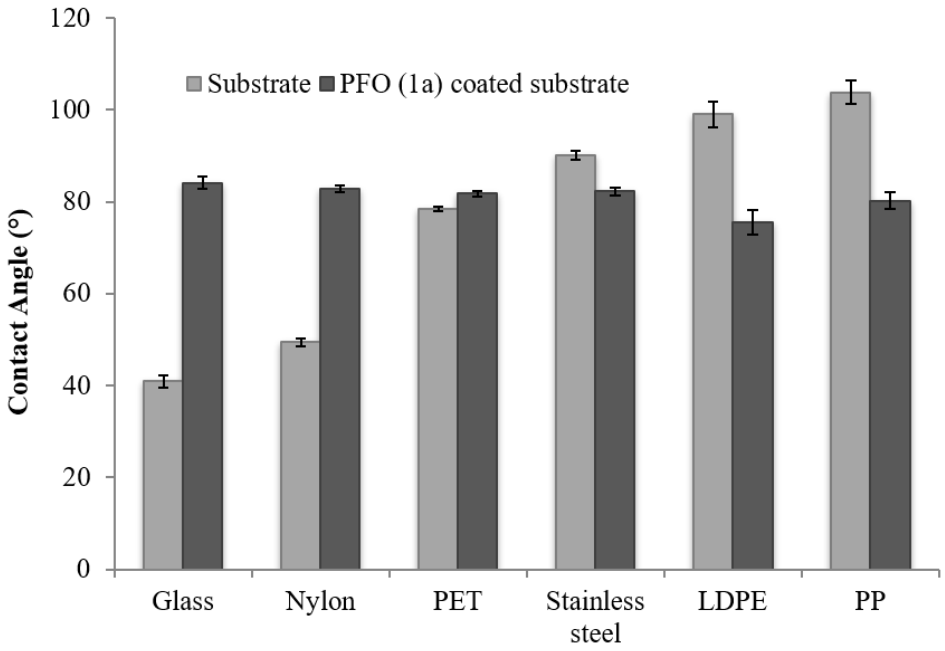

Figure 4. Contact angle measurements for uncoated glass, nylon 6,6, PET, stainless steel, LDPE and PP (blue) and PFO **1a** coated substrates (purple), showing the change in the hydrophobicity of the substrate following the application of a thin coating (24 μm) of the PFO **1a**. Error bars were calculated from standard deviations over 6 repeat measurements.

The surface free energies of the coated substrates were calculated from the contact angle data according to the model developed by Fowkes [22,23], as refined by Owens and Wendt [24], Rabel [25] and Kaelble (referred to as the OWRK model) [26]. Substrates coated with PFO **1a** were thus studied using water, ethylene glycol and 1-bromonaphthalene to provide contact angle measurements for two polar solvents and one dispersive solvent with known surface energies. The surface free energy values calculated for the films of PFO **1a** coated onto different substrates were found to be fairly consistent (37.8–39.4 mN m^{-1}) except for PFO-coated LDPE which exhibited a surface energy of 44.5 mN m^{-1} (Table 2).

Table 2. Surface energies (γ^{tot}**)** and average contact angles (°) for glass, nylon, PET, steel, LDPE and PP substrates, and for these substrates coated with films of PFO **1a**.

	Substrate					
	Glass	**Nylon 6,6**	**PET**	**Steel**	**LDPE**	**PP**
Uncoated substrate γ^{tot} (mN m^{-1})	53.3	42.8	43.8	34.6	32.4	25.7
PFO 1a coated substrate γ^{tot} (mN m^{-1})	38.5	38.7	37.8	39.0	44.5	39.4
Percentage change γ^{tot} (%)	–27.8	–9.5	–13.7	+12.7	+37.3	+53.3
Uncoated substrate water contact angle (°)	41	49	78	90	99	104
PFO 1a coated water contact angle (°)	84	83	82	82	76	80
Percentage change in contact angle (%)	+104.9	+69.4	+5.1	–8.9	–23.2	–23.1

The uncoated glass substrate exhibited the highest surface energy (53.3 mN m^{-1}) as a result of the high concentration of polar groups (typically Si-OH) on the surface of the substrate. Coating a film of PFO **1a** onto the glass substrate lowered the surface energy by –27.8%, giving a much more hydrophobic surface with a water contact angle (84°), more than twice that observed for uncoated glass (41°). The surface energies of the nylon 6,6 and PET substrates (42.8 and 43.8 mN m^{-1}, respectively) also exhibited a noticeable decrease upon coating with PFO **1a** (by –9.5 and –13.7%, respectively). Materials containing fluorocarbinol functionalities are known to minimise the surface energy of cast films by enriching the polymer-air interface with trifluoromethyl groups [9,16], which evidently accounts for the hydrophobic surface-character of the present coatings.

However, the coating of PFO **1a** on LDPE exhibited a higher surface energy (44.4 mN m^{-1}) than did coatings on most other substrates (38.7 ± 0.9 mN m^{-1}) and a correspondingly lower contact angle (76°) than on the other surfaces (80-84°). It might have been expected that PP, having a similarly non-polar surface to PE [27, 28] would show a similar trend to that

observed for PFO-coated LDPE but, as shown in Table 2, uncoated PP has an even lower surface energy (25.7 mN m^{-1}) than LDPE (32.4 mN m^{-1}). This suggests that the coating on LDPE has a different character possibly due to increased surface roughness.

The water contact angles of the lower molecular weight polymer films (PFOs **1b**–**e**) with water were also investigated, to determine whether the molecular weight of the polymer affected the surface-properties of the coating. These studies showed that the surface-hydrophobicity of the polymer was essentially unaffected by changes in molecular weight, with only minor variations (*ca*. 1°) in the contact angles measured (Table 3).

Table 3. Water contact angle measurements for PFOs **1a-e** and their precursor polymers. Angles shown are the average of six repeat measurements.

PEKK	**2a**	**2b**	**2c**	**2d**	**2e**
Contact angle (°)	98	94	95	95	96
PSE	**5a**	**5b**	**5c**	**5d**	**5e**
Contact angle (°)	106	105	103	104	105
PFO	**1a**	**1b**	**1c**	**1d**	**1e**
Contact angle (°)	88	88	88	89	88

2.3 Inkjet printing studies

The PFOs were printed using a DOD printhead purely as a screening study, before investigating their suitability as CIJ binders. The use of DOD as a screening technique permitted the use of a much smaller ink volume (3 mL) compared to that required for CIJ testing (100 mL). Before PFO **1a** could be deposited via the drop-on-demand (DOD) inkjet process it was important to determine the viscosity of the formulation to ensure that it fell within a suitable range (2–12 cP) for the Dimatix™ printhead employed in this study. The viscosities at various loadings (100, 75 and 50 mg mL^{-1}) of PFO **1a** in MEK were thus recorded at both room temperature (25 °C) and jetting temperature (42 °C) (Figure 5a). The most concentrated solution proved to be too viscous (17.5 cP) for inkjet deposition whereas lower loadings of **1a** gave viscosities within the required range. The viscosities of the different PFOs **1a-e** at a fixed concentration (100 mg mL^{-1} in MEK) were also assessed at

two different temperatures, and a clear correlation of solution viscosity with molecular weight was evident (Figure 5b).

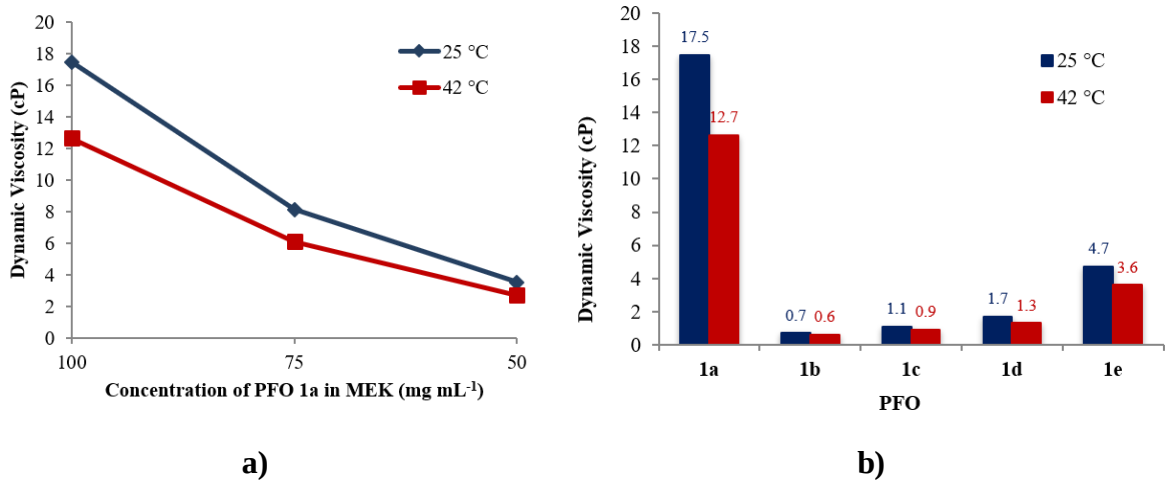

a) **b)**

Figure 5. a) Viscosities of poly(fluorocarbinol) **1a** in MEK at concentrations of 100, 75 and 50 mg mL^{-1} at 25 °C and 42 °C (a typical continuous-inkjet jetting temperature); b) viscosities of PFOs **1a-e** showing the increase in viscosity as the molecular weight of the PFO is increased.

A concentration of PFO **1a** of 50 mg mL^{-1} was selected as optimum for drop-on-demand printing as its viscosity of 3.5 cP allowed a large enough margin for the addition of a humectant without exceeding the optimum jetting viscosity. Drop-on-demand printing cannot be achieved in pure MEK because this highly volatile solvent will evaporate at the nozzle, leading to blockage. Generally, carrier solvents with boiling points above 100 °C are preferred, and di(propylene glycol) dimethyl ether (b.p. 190 °C) was thus used as a humectant with MEK (1:1 v/v): the printability of polymer **1a** was tested using the Dimatix™ DOD printhead [29]. Different cartridge temperatures and voltages were employed to find the optimum print settings, but the polymer solution did not print at all below 40 V (maximum voltage) and even *at* the maximum voltage only a small amount of material was deposited before printing failed (see SD, Table S1). The very high MW PFO **1a** was therefore not suitable for inkjet deposition, despite its solubility and relatively low viscosity in solution. It was concluded that the high molecular weight (M_n = 114,500 g mol^{-1}) of this material prohibited successful jetting as a result of elastic stresses originating from elongational flow in the nozzle [1,30,31]. Viscoelastic polymeric fluids under this deformation exhibit a complex rheological response [32,33], and at high elongational flow the formation of an elastic strand occurs and elastic stresses dominate, leading to a non-Newtonian increase in

viscosity, nozzle blockage, and failure to print. However, the high polarity and excellent solubility of the lower-MW PFOs **1b-e** warranted their investigation as potential inkjet materials, and studies were carried out using the Dimatix™ DOD printhead at a polymer concentration of 100 mg mL^{-1} in MEK:di(propylene glycol) dimethyl ether, (1:1 v/v). All four PFOs were successfully deposited onto sheen card, with the optimum printing conditions varying for the different molecular weight materials (SD, Table S2). The high molecular weight PFO, **1e** (M_n = 44,900 g mol^{-1}), printed successfully at a cartridge voltage of 40 V but not at lower voltages. In contrast, PFOs **1b** (M_n = 11,500 g mol^{-1}) and **1c** (M_n = 19,100 g mol^{-1}) gave optimum jetting at 30 V and, although **1d** (M_n = 25,200 g mol^{-1}) was also printable at 30 V, a sharper image was produced at 35 V.

In the light of these initial screening studies, two of the five PFOs (**1b** and **1d**) were selected for scale up and deposition analysis in continuous inkjet (CIJ) printing mode. The lowest MW PFO **1b** was selected as it was likely to pose the lowest risk of nozzle blockage [1,30,31] and PFO **1d** was chosen because, although its molecular weight is more than double that of **1b**, it had still printed well under DOD conditions.

The dynamic viscosities of PFOs **1b** and **1d** (formulated at 100 mg mL^{-1} in MEK) were 0.7 and 1.7 cP, respectively, which are lower than optimum for continuous inkjet (CIJ) printing. Polymer concentrations were therefore increased in the formulations of **1b** (300 mg mL^{-1}) and **1d** (200 mg mL^{-1}), giving solution viscosities of 5.3 and 3.9 cP respectively (Figure 6).

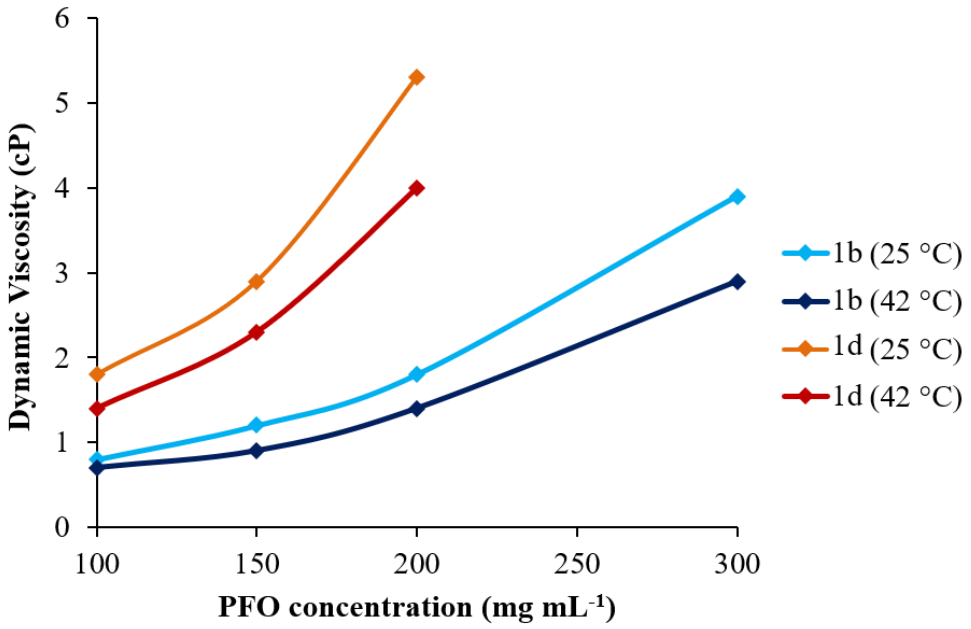

Figure 6. Dynamic viscosities of polymers **1b** and **1d** at different concentrations in MEK having appropriate viscosity (3–6 cP) for CIJ inkjet deposition [200 mg mL^{-1} and 300 mg mL^{-1} for polymers **1d** (5.3 cP at 25 °C) and **1b** (3.9 cP at 25 °C), respectively].

The addition of polymers to inkjet formulations can alter the Newtonian behaviour of the carrier solvent, as the polymer chains disentangle, align and stretch upon ejection from the nozzle (typically some 60 µm in diameter) at high shear rates. Thus, the rheological behaviour of polymers, as they pass through the printhead, is an important factor that defines the suitability of polymers for CIJ printing as this technology involves the recirculation of ink through the nozzle many times. The high shear rates, observed in CIJ printing, can be simulated in shear rheology measurements which allow assessment of polymer chain alignment in a high shear environment. High shear rheology on the formulations of **1b** and **1d** as they passed through a microchannel at various shear rates showed that PFO **1b** behaved as a Newtonian fluid under these test conditions, and **1d** exhibited near-Newtonian behaviour with only a minor amount of shear thickening – increase in viscosity of 0.13 cP – as the shear rate was increased (Figure S44).

Promisingly, the near-Newtonian behaviour of polymers **1b** and **1d** indicated that these materials should be suitable for deposition under the CIJ deposition regime as employed in high-throughput industrial printing systems.

Ink formulations for use in high-throughput CIJ printers must possess a charge to facilitate sufficient deflection from the charge electrode onto the substrate and therefore in the prototype PFO samples addition of a conductive dye was required. In this study the ionic, metal-complex dye Orasol® orange 247 was found to provide good conductivity (772 and 804 µS cm^{-1} for **1b** and **1d**, respectively) at relatively low concentration (4 wt%) and aided visualisation of the prints.

The break-up of the jetstream of formulations of **1b** and **1d** in MEK with Orasol® orange 247 was studied with the aid of a strobe light operating at 85 kHz. The images show good breakup of the jet stream, with small tails on the droplets recombining with the main droplets further down the stream, without the formation of satellite drops (Figure 7).

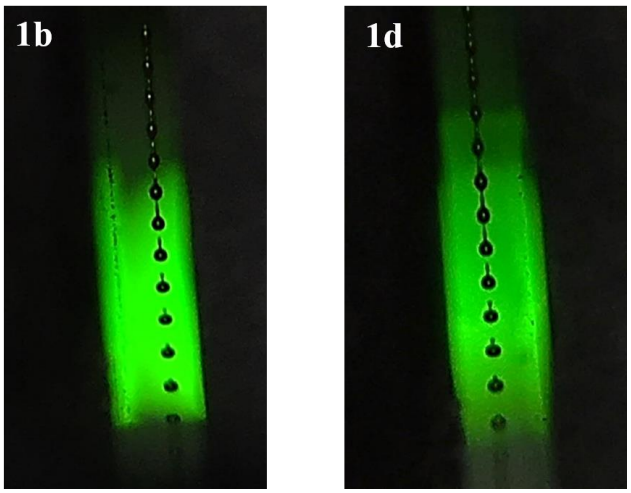

Figure 7. Droplet formation during CIJ printing of formulations of polymers **1b** and **1d**, obtained using an 85 kHz stroboscopic light.

The formulations of PFOs **1b** and **1d** were both deposited successfully from a CIJ printhead (set at 42 °C) onto a variety of substrates at ambient temperature including glass, nylon, PET, stainless steel, LDPE and PP using a Domino Ax-series CIJ printer, and produced clear, well-defined images without any apparent satellite drops or misplaced drops (Figure 8).

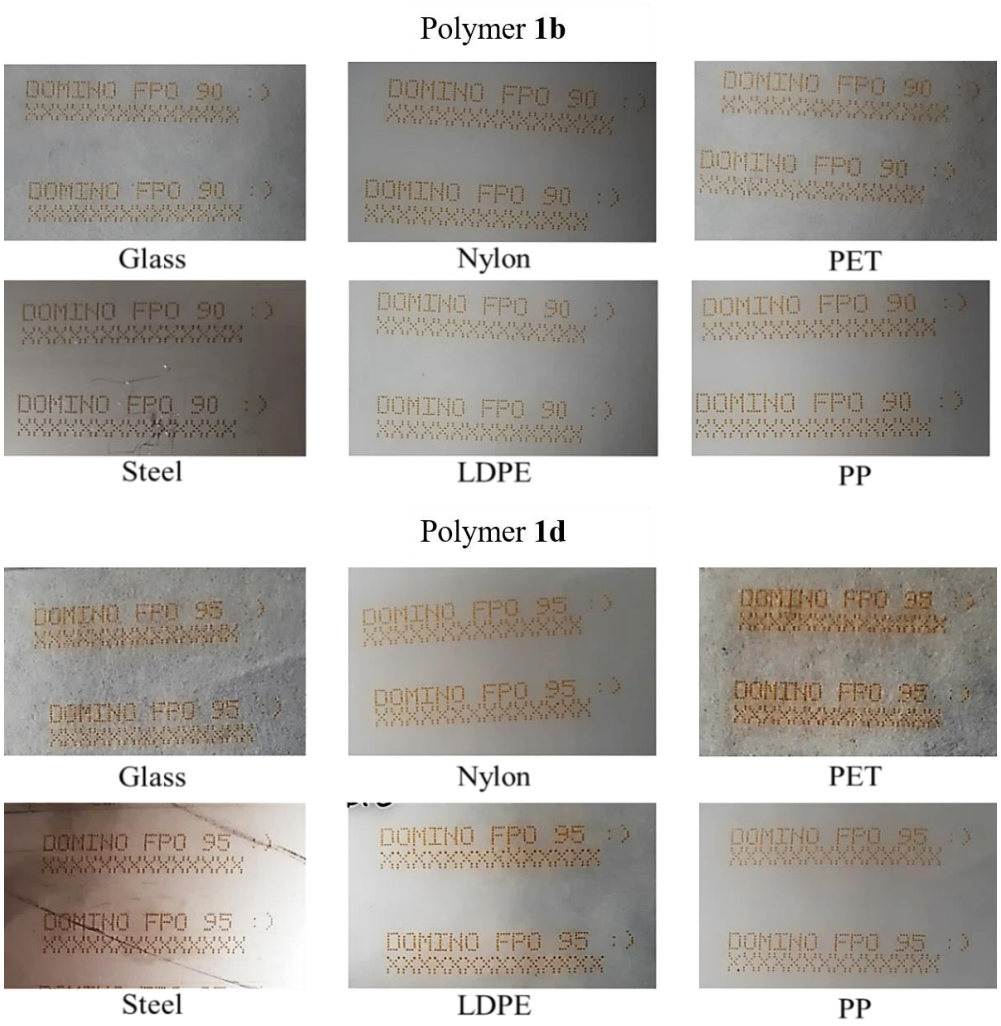

Figure 8. Results of CIJ deposition of PFO samples **1b** and **1d** onto glass, nylon, PET, stainless steel, LDPE and PP showing clear printed code in all cases. The high quality of the prints produced using these polymers can be seen in the enlarged images given in the Supplementary Data (Figure S45).

The adhesion of the polymer/dye coating to the substrates was then evaluated using peel tests. Adhesive tape (810 grade) was used and the amount of material removed from the substrate was rated from 1–5, where 1 indicates the complete removal of the print (very poor adhesion) and 5 indicates no removal of print (e.g. excellent adhesion). Both of the deposited PFO samples exhibited very poor adhesion to PP, as this substrate possesses a very low surface energy (25.7 mNm^{-1}, see Table 2), and most likely results from poor wetting of the substrate [27,28]. The PFO polymers exhibited moderately good adhesion to steel and, more promisingly, excellent adhesion to glass, nylon and PET (Table 4). The durability of CIJ-printed images on steel was also tested using a steam-retort. The prints remained in place after an hour's exposure to steam, although some leaching of the dye was observed.

Table 4. Adhesion of polymers **1b** and **1d** to different substrates, where 1 = very poor adhesion and 5 = excellent adhesion.

	Substrate					
Sample	**Glass**	**PET**	**Nylon**	**Steel**	**LDPE**	**PP**
1b	5	5	5	3	1	1
1d	4	5	5	3	1	1

The results obtained in this study indicate that polymers **1b** and **1d** are soluble, printable, and demonstrate hydrophobic properties post-deposition. These materials show Newtonian or near-Newtonian behaviour, and there seems little or no risk of their causing nozzle blockage in a commercial CIJ printing system. Overall, the results clearly indicate that the materials have potential as surface-hydrophobic polymer binders for inkjet formulations, which are yet readily soluble in the high-polarity solvents preferred for inkjet printing. Regarding the safety of these materials, no long-term toxicology studies have yet been undertaken, but their high molecular weights suggest that migration through packaging films and/or cell membranes would be extremely limited. In terms of sustainability, the quantities of polymers consumed in inkjet printing are minute in comparison to those used in, for example, packaging or construction, so that use of the present polymers in this context would have only a negligible effect on natural resources.

3. Conclusions

A series of five aromatic poly(ether-ketone)s (PEKKs **2a**–**e**) with a range of different molecular weights have been synthesised by varying the stoichiometric ratio of monomers used in the AA/BB-type step-growth polymerisation. The PEKKs were converted successfully to readily-soluble poly(fluorocarbinol)s (PFOs **1a**–**e**) (M_n = 11,500–114,500 g mol^{-1}) via their poly(silyl ether) derivatives (PSEs **5**a–e). The surface characteristics of cast PFO films, investigated using contact angle measurements, revealed a consistent surface-hydrophobicity (water contact angle 88–89°) that was independent of the molecular weight of the poly(fluorocarbinol).

Inkjet printing studies of the PFOs using a DOD printhead showed that the highest molecular weight polymer, **1a**, (M_n = 114,500 g mol^{-1}) was not printable, as a result of elastic stress

from the elongational flow which is often observed in high molecular weight polymer formulations. The lower-MW PFOs (**1b**–**e**) were deposited successfully, but PFO **1e (**M_n = 44,900 g mol^{-1}) required maximum voltage of the piezoelectric printhead during deposition, indicating the highest risk of print failure in this series.

Polymers **1b** (M_n = 11,500) and **1d** (M_n = 25,200) were investigated further for their potential in continuous-inkjet (CIJ) formulations, and pre-CIJ deposition screening suggested that both materials would be suitable for CIJ printing. Polymer **1b** acted as a Newtonian fluid under high-shear jetting conditions and **1d** exhibited only a small degree of shear-thickening (near-Newtonian fluid), indicating minimal risk of viscosity modification during printing. Polymers **1a** and **1d** were both deposited using a Domino Ax-series CIJ printer and demonstrated good drop break-up, further indicating their suitability as inkjet materials. Both polymers were deposited successfully onto a variety of substrates, including PET, Nylon 6,6 and glass, to which the polymers demonstrated good adhesion, confirming their potential as polymeric binders.

The poly(fluorocarbinols)s **1b** and **1d** are thus suitable polymer additives for inkjet formulations, with both materials showing good solubility, jettability, adhesion and hydrophobic surface-properties. It was concluded that polymer **1b** demonstrates the more favourable characteristics for use in an inkjet formulation, since it behaves as a Newtonian fluid in the printhead.

4. Experimental

For full experimental details see the Supplementary Data.

5. Acknowledgements

We thank EPSRC and Domino Printing Sciences UK Ltd. for a PhD studentship in support of JG. Spectroscopic and thermal analytical data were acquired using equipment in the Chemical Analysis Facility (CAF) of the University of Reading. Facilities for printing of polymer samples and contact angle measurements were provided by Domino Printing Sciences UK Ltd., Bar Hill, Cambridge, UK. We thank EPSRC for a Platform Grant (EP/L020599/1) that supported FL.

6. References

[1] A.S. Johns, C.D. Bain, Ink-jet printing of high-molecular-weight polymers in oil-in-water emulsions, ACS Appl. Mater. Interfaces. 9 (2017) 22918–22926. https://doi.org/10.1021/acsami.7b04454.

[2] J.S.R. Wheeler, S.G. Yeates, Polymers in inkjet printing In: Fundamentals of Inkjet Printing, (2015), Wiley, Weinheim pp.117–140. https://doi.org/10.1002/9783527684724.ch5.

[3] D. Xu, V. Sanchez-Romaguera, S. Barbosa, W. Travis, J. De Wit, P. Swan, S.G. Yeates, Inkjet printing of polymer solutions and the role of chain entanglement, J. Mater. Chem. 17 (2007) 4902–4907. https://doi.org/10.1039/b710879f.

[4] Y. Christanti, L.M. Walker, Effect of fluid relaxation time of dilute polymer solutions on jet breakup due to a forced disturbance, J. Rheol. 46 (2002) 733–748. https://doi.org/10.1122/1.1463418.

[5] O.A. Basaran, H. Gao, P.P. Bhat, Nonstandard inkjets, Annu. Rev. Fluid Mech. 45 (2013) 85–113. https://doi.org/10.1146/annurev-fluid-120710-101148.

[6] H.J. Spinelli, Polymeric dispersants in ink jet technology, Adv. Mater. 10 (1998) 1215–1218. https://doi.org/10.1002/(SICI)1521-4095(199810)10:15<1215::AID-ADMA1215>3.0.CO;2-0.

[7] Z. Zołek-Tryznowska, J. Izdebska, Flexographic printing ink modified with hyperbranched polymers: Boltorn™ P500 and Boltorn™ P1000, Dye. Pigment. 96 (2013) 602–608. https://doi.org/10.1016/j.dyepig.2012.10.003.

[8] R.P. Mun, J.A. Byars, D. V. Boger, The effects of polymer concentration and molecular weight on the breakup of laminar capillary jets, J. Non-newtonian. Fluid Mech. 74 (1998) 285–297. https://doi.org/10.1016/S0377-0257(97)00074-8.

[9] A. Hirao, K. Sugiyama, H. Yokoyama, Precise synthesis and surface structures of architectural per- and semifluorinated polymers with well-defined structures, Prog. Polym. Sci. 32 (2007) 1393–1438. https://doi.org/10.1016/j.progpolymsci.2007.08.001.

[10] S. Banerjee, B. V. Tawade, V. Ladmiral, L.X. Dupuy, M.P. MacDonald, B. Améduri, Poly(fluoroacrylate)s with tunable surface hydrophobicity via radical copolymerization of 2,2,2-trifluoroethyl α-fluoroacrylate and 2-(trifluoromethyl)acrylic acid, Polym. Chem. 8 (2017) 1978–1988. https://doi.org/10.1039/C7PY00209B.

[11] Y. Patil, B. Ameduri, Progress in Polymer Science Advances in the (co) polymerization of alkyl 2-trifluoromethacrylates and 2- (trifluoromethyl) acrylic acid, Prog. Polym. Sci. 38 (2013) 703–739.

https://doi.org/10.1016/j.progpolymsci.2012.09.005.

[12] M. Damaceanu, C. Constantin, A. Nicolescu, M. Bruma, N. Belomoina, R.S. Begunov, Highly transparent and hydrophobic fluorinated polyimide films with ortho -kink structure, Eur. Polym. J. 50 (2014) 200–213. https://doi.org/10.1016/j.eurpolymj.2013.10.030.

[13] M. Tamura, R. Chaiwattananone, A. Sekiya, new type thin films of polymers modified with triftuoromethyl and long chain perfluoroalkyl groups spread on the water surface, Polym. J. 24 (1992) 1307–1309.

[14] B. Liu, G. Wang, W.E.I. Hu, Y. Jin, C. Chen, Z. Jiang, W. Zhang, Z. Wu, Y.E.N. Wei, Poly(aryl ether ketone) s with (3-methyl)phenyl and (3-trifluoromethyl)phenyl side groups, J. Polym. Sci. Part A Polym. Chem. 40 (2002) 3392–3398. https://doi.org/10.1002/pola.10434.

[15] I. Ruppert, K. Schlich, W. Volbach, Die Ersten CF3-substituierten organyl(chlor)silane, Tetrahedron. 25 (1984) 2195–2198.

[16] F. Leroux, R.A. Bennett, D.F. Lewis, H.M. Colquhoun, Trifluoromethylation of carbonyl groups in aromatic poly(ether ketone)s: formation of strongly polar yet surface-hydrophobic poly(arylenenecarbinol)s, Macromolecules. 51 (2018) 3415–3422. https://doi.org/10.1021/acs.macromol.8b00017.

[17] G.K.S. Prakash, A.K. Yudin, Perfluoroalkylation with organosilicon reagents, Chem. Rev. 97 (1997) 757–786. https://doi.org/10.1021/cr9408991.

[18] G.K.S. Prakash, R. Krishnamurti, G.A. Olah, Fluoride-induced trifluoromethylation of carbonyl compounds with trifluoromethyltrimethylsilane (TMS-CF3). A trifluoromethide equivalent, J. Am. Chem. Soc. 111 (1989) 393–395. https://doi.org/10.1021/ja00183a073.

[19] R.P. Singh, G. Cao, R.L. Kirchmeier, J.M. Shreeve, Cesium fluoride catalyzed trifluoromethylation of esters, aldehydes, and ketones with (trifluoromethyl)trimethylsilane, J. Org. Chem. 64 (1999) 2873–2876. https://doi.org/10.1021/jo982494c.

[20] R.P. Singh, R.L. Kirchmeier, J.M. Shreeve, TBAF-catalyzed direct nucleophilic trifluoromethylation of α-keto amides with trimethyl(trifluoromethyl)silane, J. Org. Chem. 64 (1999) 2579–2581. https://doi.org/10.1021/jo982297d.

[21] R. Krishnamurti, D.R. Bellew, G.K.S. Prakash, Preparation of trifluoromethyl and other perfluoroalkyl compounds with (perfluoralkyl)trimethylsilanes, J. Org. Chem. 56 (1991) 984–989. https://doi.org/10.1021/jo00003a017.

[22] F.M. Fowkes, Attractive forces at interfaces, Ind. Eng. Chem. 56 (1964) 40–52. https://doi.org/10.1021/ie50660a008.

[23] F.M. Fowkes, Calculation of work of adhesion by pair potential summation, J. Colloid Interface Sci. 28 (1968) 493–505. https://doi.org/10.1016/0021-9797(68)90082-9.

[24] D.K. Owens, R.C. Wendt, Estimation of the surface free energy of polymers, J. Appl. Polym. Sci. 13 (1969) 1741–1747. https://doi.org/10.1002/app.1969.070130815.

[25] W. Rabel, Einige aspekte der benetzungstheorie und ihre anwendung auf die untersuchung und veränderung der oberflächeneigenschaften von polymeren., Farbe Und Lack. 77 (1971) 997–1005.

[26] D.H. Kaelble, Dispersion-polar surface tension properties of organic solids, J. Adhes. 2 (1970) 66–81. https://doi.org/10.1080/0021846708544582.

[27] D.M. Mattox, Substrate ("real") surfaces and surface modification, in: Handbook of Physical Vapor Deposition Processes, (1998) William Andrew, New York, pp. 56–126. https://doi.org/10.1016/b978-081551422-0.50003-6.

[28] J. Balart, V. Fombuena, J.M. España, L. Sánchez-Nácher, R. Balart, Improvement of adhesion properties of polypropylene substrates by methyl methacrylate UV photografting surface treatment, Mater. Des. 33 (2012) 1–10. https://doi.org/10.1016/j.matdes.2011.06.069.

[29] FUJIFILM Inc., Dimatix™ Materials Printer DMP-2800 Series User Manual, 2010, 4th Edition, pp 1-150.

[30] B.J. De Gans, E. Kazancioglu, W. Meyer, U.S. Schubert, Ink-jet printing polymers and polymer libraries using micropipettes, Macromol. Rapid Commun. 25 (2004) 292–296. https://doi.org/10.1002/marc.200300148.

[31] B.J. de Gans, P.C. Duineveld, U.S. Schubert, Inkjet printing of polymers: state of the art and future developments, Adv. Mater. 16 (2004) 203–213. https://doi.org/10.1002/adma.200300385.

[32] S.J. Haward, G.H. Mckinley, A.Q. Shen, Elastic instabilities in planar elongational flow of monodisperse polymer solutions, Nat. Sci. Reports. 6 (2016) 1–18. https://doi.org/10.1038/srep33029.

[33] I. Delaby, R. Muller, B. Ernst, Drop deformation during elongational flow in blends of viscoelastic fluids. Small deformation theory and comparison with experimental results, Rheol. Acta. 34 (1995) 525–533. https://doi.org/10.1007/BF00712313.